Environmental Science & Technology

pubs.acs.org/est

Article

Direct and Indirect Effects of Increased CO_2 Partial Pressure on the Bioenergetics of Syntrophic Propionate and Butyrate Conversion

Pamela Ceron-Chafla,* Robbert Kleerebezem, Korneel Rabaey, Jules B. van Lier, and Ralph E. F. Lindeboom

Cite This: *Environ. Sci. Technol.* 2020, 54, 12583−12592

Read Online

ACCESS | Metrics & More | Article Recommendations | Supporting Information

ABSTRACT: Simultaneous digestion and in situ biogas upgrading in high-pressure bioreactors will result in elevated CO_2 partial pressure (pCO_2). With the concomitant increase in dissolved CO_2, microbial conversion processes may be affected beyond the impact of increased acidity. Elevated pCO_2 was reported to affect the kinetics and thermodynamics of biochemical conversions because CO_2 is an intermediate and end-product of the digestion process and modifies the carbonate equilibrium. Our results showed that increasing pCO_2 from 0.3 to 8 bar in lab-scale batch reactors decreased the maximum substrate utilization rate (r_{smax}) for both syntrophic propionate and butyrate oxidation. These kinetic limitations are linked to an increased overall Gibbs free energy change ($\Delta G_{Overall}$) and a potential biochemical energy redistribution among syntrophic partners, which showed interdependence with hydrogen partial pressure (pH_2). The bioenergetics analysis identified a moderate, direct impact of elevated pCO_2 on propionate oxidation and a pH-mediated effect on butyrate oxidation. These constraints, combined with physiological limitations on growth exerted by increased acidity and inhibition due to higher concentrations of undissociated volatile fatty acids, help to explain the observed phenomena. Overall, this investigation sheds light on the role of elevated pCO_2 in delicate biochemical syntrophic conversions by connecting kinetic, bioenergetic, and physiological effects.

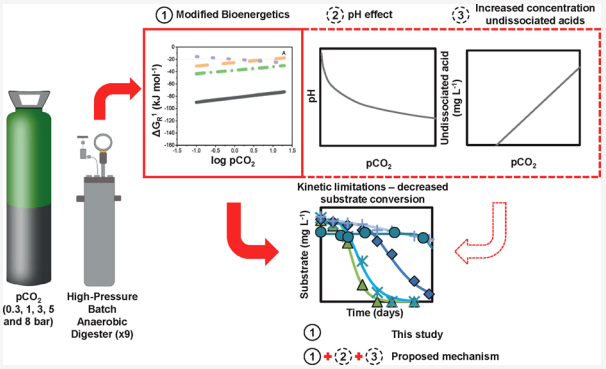

INTRODUCTION

High-pressure anaerobic digestion (HPAD) has been proposed as a technology for in situ biogas upgrading,[1−3] able to achieve a CH_4 content >90%, after which the produced CH_4 is in principle suitable for further direct use in, for example, (decentralized) gas grid injection or advanced industrial processes. HPAD takes advantage of the large difference in solubility between CH_4 and CO_2, which is most pronounced at high pressures in a digester equipped with a pressure valve for biogas release. However, by letting the pressure rise, the CH_4 content increases in the headspace, whereas CO_2 and other ionizable gases such as H_2S dissolve in the liquid. Thus far, the effects of increased dissolved CO_2 on the overall performance of the high-pressure system have hardly been studied beyond accumulating acidity.[4] As far as the authors are aware, limited attention has been paid to its possible impact on metabolic conversion routes and degradation rates.

CO_2 has multiple roles in biological systems such as electron acceptor, carbon donor, intermediate, and end-product of biochemical reactions, and contributes to the aquatic buffer system via the carbonate equilibrium.[5] These multiple roles complicate studies searching for a mechanistic description of the response to increased CO_2 partial pressure (pCO_2) in natural and engineered environments, except for the bacteriostatic effects of high pCO_2 applied for sterilization purposes at 40−300 bar and 20−50 °C. The bacteriostatic action leads to cytoplasm acidification, cell rupture, and inactivation of key enzymes and transport proteins.[6−8] The impact of "moderate" pCO_2 from 0.1 up to 10 bar is less comprehensively described and is mainly attributed to a decreased intracellular pH.[9] However, pH reduction by itself does not explain the reduced microbial activity of denitrifying bacteria observed by Wan et al.[10] because of dissolved CO_2 concentrations up to 30,000 ppm. These authors proposed that elevated pCO_2 caused direct inhibition of the carbon metabolism, electron transport chain, enzymatic activity, and substrate consumption at the expense of increased buffer concentration to prevent a pH drop.[10,11]

Received: April 1, 2020
Revised: August 25, 2020
Accepted: August 26, 2020
Published: August 26, 2020

https://dx.doi.org/10.1021/acs.est.0c02022
Environ. Sci. Technol. 2020, 54, 12583−12592

Research on the impact of moderate pCO_2 on methanogenesis is limited to observations relevant to oil reservoirs. Operational conditions of 50 bar pressure, 10% pCO_2, and temperature of 55 °C resulted in a shift from syntrophic acetate oxidation (SAO) to aceticlastic methanogenesis (AcM).[12] The effects of CO_2 supplementation at atmospheric pressure in anaerobic digesters (ADs) are better documented in literature; when accompanied by stoichiometric H_2 provision, it enhances CH_4 production because of promoted hydrogenotrophic methanogenesis (HyM).[13] Also, exogenous CO_2 can be indirectly converted to CH_4 via homoacetogenesis coupled to AcM. This mechanism has been proposed to explain the increased CH_4 production after CO_2 direct injection in (a) pilot-scale AD treating food waste[14,15] and (b) two-phase AD-treating sewage. The accompanying. The accompanying electron donor was not highlighted; nonetheless, this role could be performed by additional H_2 coming from enhanced acidogenesis[15] or after the release of other hydrolyzed material from cell lysis.[16]

Increased CO_2 also induces changes in microbiome activity, diversity, community structure, and microbial interactions.[8] The last one is of vital importance in ADs, which rely on syntrophy to overcome thermodynamic limitations for the conversion of intermediate compounds, namely propionate and butyrate.[17,18] The accumulation of these intermediates correlates with reactor disturbance because of the increased organic loading rate, pH changes, and unpaired acidogenesis and methanogenesis.[19] Since these conversions operate close to thermodynamic equilibrium, subtle variations in substrate/product concentrations and environmental conditions can modify the actual Gibbs free energy change (ΔG_R^1) of a specific pathway.[20] The effects of elevated CO_2 on syntrophic interactions have been studied in subsurface environments destined for geological carbon storage.[21,22] Bioenergetic simulations have shown different outcomes on the ΔG_R^1 of the intermediate reactions: the energetic feasibility of substrate oxidation and aceticlastic methanogenic conversions decreased, whereas the contrary occurred for HyM.[22,23] As a consequence of the apparent thermodynamic control exerted by pCO_2, specific bacterial metabolisms might be promoted or inhibited.[24]

In our present work, we studied the impact of elevated pCO_2 on the kinetics and bioenergetics of the syntrophic conversion of propionate and butyrate. It is hypothesized that an increase in the overall available Gibbs free energy for substrate conversion, because of increased pCO_2, could provoke an imbalance in the energy share among syntrophic partners that might translate into kinetic limitations. A scenario analysis is proposed to understand the individual and combined effects of pCO_2 and pH on the bioenergetics of syntrophic conversions. Furthermore, the relationship between bioenergetic and kinetic data is evaluated through a correlation analysis aiming to provide insight into the system response to changing available energy.

MATERIALS AND METHODS

Experimental Setup and Reactor Operation. Five initial operational pCO_2, that is, 0.3, 1, 3, 5, and 8 bar, were selected for the experimental treatments based on pH equilibrium calculations performed with the hydrogeochemical software PHREEQC (version 3, USGS). The application of an elevated buffer concentration of 100 mM as HCO_3^- in the system allowed to maintain circumneutral pH, despite the elevated pCO_2. Batch experiments at 0.3 and 1 bar were carried out at atmospheric pressure in 250 mL Schott bottles sealed with rubber stoppers. In parallel, the elevated pressure experiments were performed in 200 mL stainless-steel pressure-resistant reactors (Nantong Vasia, China). The experiments were conducted at a liquid: gas ratio of 1.5:1 and inoculum/substrate ratio of 2:1 g COD g VSS^{-1}. The liquid medium consisted of macronutrient and micronutrient stock solutions (6 and 0.6 mL L^{-1}, respectively) prepared according to Lindeboom et al.[1] and 1 g of COD L^{-1} of the substrates propionate or butyrate.

The headspace of bottles and reactors was replaced with N_2 gas (>99%) to ensure anaerobic conditions after filling. Then, the bottles were flushed with the corresponding gas mixture: 70:30% N_2/CO_2 for 0.3 bar pCO_2 or >99% CO_2 for 1 bar pCO_2. Elevated pressure reactors were subjected to three consecutive pressurization-release cycles to ensure complete N_2 replacement by CO_2 (>99%) at the intended pressure. Temperature and agitation speed were controlled using an incubator shaker (Innova 44, Eppendorf, USA) set to 35 ± 1 °C and 110 ± 10 rpm. Pressure was online-monitored using digital sensors (B + B Thermo-Techniek, Germany) and a microcontroller (Arduino Uno, Italy). The experiments had a fixed duration of 14 days.

Inoculum Selection. Preliminary experiments of propionate anaerobic conversion under 1 bar pCO_2 were conducted in triplicates using three mesophilic inocula collected from (A) sludge digester-treating excess sewage sludge, (B) UASB reactor-treating sugar beet wastewater, and (C) anaerobic membrane bioreactor-treating food industry wastewater. The three inocula were characterized in terms of physicochemical parameters (Supporting Information, Table S1), and inoculum C was selected for the experiments here described (Supporting Information, Figure S1).

Analyses. Experiments were carried out in triplicate incubation; however, because of the small working volume of the reactors (200 mL), a sampling strategy for liquid and gas samples was designed that enabled us to account for replicate variability, minimizing disturbance of the batch incubations (Supporting Information, Table S2). Headspace composition and volatile fatty acids (VFAs) were analyzed using gas chromatography (7890A GC system, Agilent Technologies, US). In the first one, gas samples (5 mL) taken two times per week at atmospheric pressure were measured via a thermal conductivity detector and directed through an HP-PLOT Molsieve GC column (30 m length × 0.53 mm inner diameter × 25 μm film thickness). Helium was used as the carrier gas at a constant flow of 10 mL min^{-1}. The oven and detector were operated at 45 and 200 °C, respectively. In the second one, VFAs were determined according to Ghasimi et al.[25] Total and soluble COD, total suspended solids, volatile suspended solids (VSS), and pH were measured at the beginning and end of the experiment according to Standard Methods.[26]

Estimation of Kinetic Parameters. The modified Gompertz equation[27]

$$y = A \times e^{[-er_{s\,max} \times e/A \times (\lambda - t) + 1]} \quad (1)$$

where y represents the substrate concentration (mg L^{-1}), λ is the lag phase (day), r_{smax} is the maximum substrate utilization rate (mg L^{-1} day^{-1}), A is the maximum substrate concentration (mg L^{-1}), and t is the time (days), was used to fit the data from the atmospheric and pressure experiments.

https://dx.doi.org/10.1021/acs.est.0c02022
Environ. Sci. Technol. 2020, 54, 12583−12592

Table 1. Stoichiometry of the Main Subreactions Related to Syntrophic Propionate and Butyrate Oxidation with Their Corresponding ΔG_R^{01} (kJ mol^{-1}) Calculated at Biochemical Standard Conditions of Temperature = 298.15 K, Concentration of Aqueous Reactants = 1 mol L^{-1}, Pressure of Gaseous Reactants = 1 bar, and pH = 7

substrate	reaction		ΔG_R^{01} (kJ mol^{-1})
propionate	overall	$C_3H_5O_2^- + H^+ + 0.5H_2O \rightarrow 1.75CH_4 + 1.25CO_2$	−60.2
	oxidation (Pr-Ox)	$C_3H_5O_2^- + 2H_2O \rightarrow C_2H_3O_2^- + 3H_2 + CO_2$	+73.7
	AcM	$C_2H_3O_2^- + H^+ \rightarrow CH_4 + CO_2$	−35.8
	HyM	$3H_2 + 0.75CO_2 \rightarrow 0.75CH_4 + 1.5H_2O$	−98.0
butyrate	overall	$C_4H_7O_2^- + H^+ + H_2O \rightarrow 2.5CH_4 + 1.5CO_2$	−88.8
	oxidation (Bu-Ox)	$C_4H_7O_2^- + 2H_2O \rightarrow 2C_2H_3O_2^- + H^+ + 2H_2$	+48.2
	AcM	$2C_2H_3O_2^- + 2H^+ \rightarrow 2CH_4 + 2CO_2$	−71.6
	HyM	$2H_2 + 0.5CO_2 \rightarrow 0.5CH_4 + H_2O$	−65.4

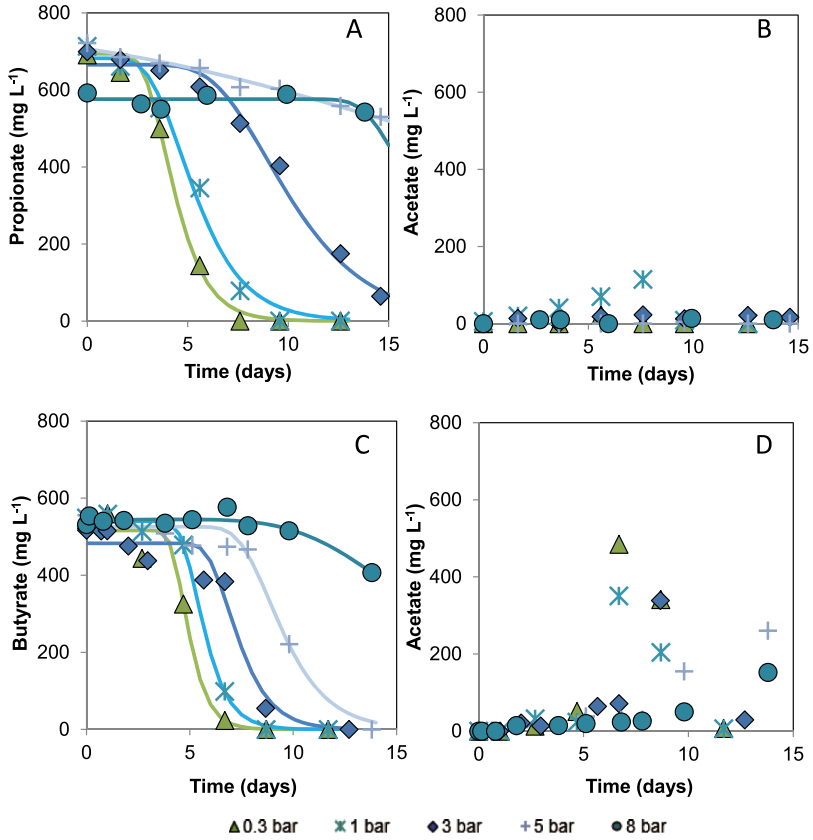

Figure 1. Evolution of substrate consumption and acetate production during mesophilic syntrophic substrate oxidation under 0.3, 1, 3, 5, and 8 bar initial pCO_2. (A,B) correspond to the propionate and acetate concentration (mg L^{-1}) for the propionate experiment, respectively. The concentrations shown in time points 0, 10, and 13 days represent the average of three sampled reactors with a relative standard deviation <16%. (C,D) correspond to the butyrate and acetate concentration (mg L^{-1}) for the butyrate experiment, respectively. The concentrations presented in time points 0, 5, and 12 days represent the average of three sampled reactors with a relative standard deviation <18%. Data points represent experimental data. Continuous lines correspond to the simulated data using the modified Gompertz equation, the significance levels of which are presented in Table 2.

The kinetic parameters were estimated using nonlinear minimization methods from the package nlstools in R (v3.6.1).[28]

Bioenergetic Calculations. ΔG_R^1, the actual Gibbs free energy change for the reactions, was calculated according to[29]

$$\Delta G_R^1 = \Delta G_R^{01} + RT\sum_{i=1}^{n} Y_{Si}^R \ln(a_{Si}) \quad (2)$$

where ΔG_R^{01} is the Gibbs free energy at pH 7 and 308.15 K, R is the gas constant (8.31 J K^{-1} mol^{-1}), T is the temperature in kelvin, Y_{Si}^R is the stoichiometric coefficient of compound i, and a_{Si} is the molar concentration of compound i. ΔG_R^{01} was corrected for temperature using the Gibbs−Helmholtz equation.[29] The values at standard conditions, ΔG_R^0, were taken from Heijnen and Kleerebezem.[30]

Estimation of Potential Biochemical Energy Distribution in Syntrophic Oxidation of Propionate and Butyrate. The stoichiometry of the overall syntrophic reaction and the intermediate catabolic reactions is presented in Table 1. From the acetotrophic reactions, only AcM was included in the analysis because SAO was considered unlikely to occur under our experimental conditions and initial community composition (Supporting Information, Figure S2). The stoichiometric coefficients of AcM and HyM for each substrate

https://dx.doi.org/10.1021/acs.est.0c02022
Environ. Sci. Technol. 2020, 54, 12583−12592

Table 2. Overview of the Kinetic Parameters Estimated Using the Modified Gompertz Equation for Propionate and Butyrate Oxidation at the Different Conditions of Initial pCO_2: 0.3, 1, 3, and 5 bar[a,b]

substrate		propionate				butyrate			
parameter	initial pCO_2 (bar)	0.3	1	3	5	0.3	1	3	5
	eq. pCO_2 (bar)	0.3	1	1.5	2	0.3	1	1.5	2.0
	eq. pH	7.4	6.9	6.4	6.2	7.4	6.9	6.4	6.2
A (mg L^{-1})		667.9***	681.8***	664.8***	587.5**	516.2***	540.1***	465.9***	525.9***
r_{smax} (mg L^{-1} day^{-1})		223.9***	149.5**	89.8***	14.4 ( )	291.2 ( )	238.9***	216.9*	126.6**
λ (day)		3.3***	3.4**	6.6***	4.7 ( )	4.3***	4.8***	6.3***	7.3***
specific r_{smax} (mg substrate g^{-1} VSS added day^{-1})		117.2	78.3	46.9	7.5	138.7	113.8	103.3	60.3

[a]The measured equilibrium pCO_2 and the calculated equilibrium pH are additionally provided. [b]Levels of significance of the parameter estimation: p-value ( ) < 0.1, * <0.05, ** <0.01, and *** <0.001.

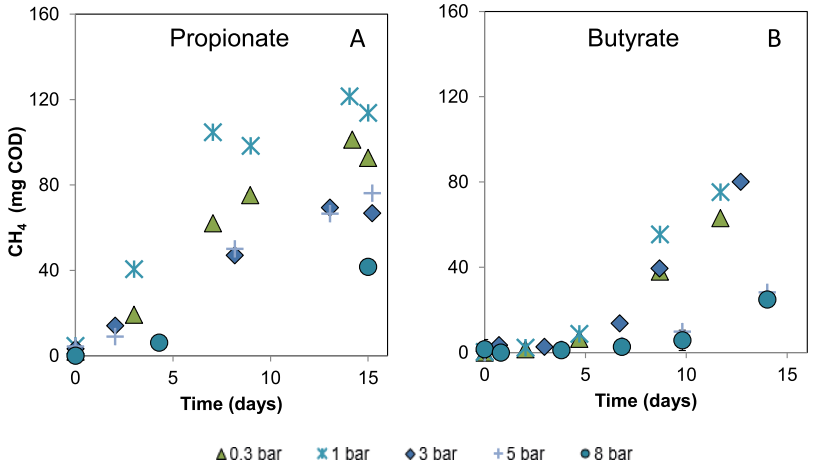

Figure 2. Evolution of methane production (mg COD) during mesophilic syntrophic substrate oxidation under 0.3, 1, 3, 5, and 8 bar initial pCO_2. Data points represent experimental data. (A) Propionate experiment. Values presented in time points 0, 10, and 13 days represent the average of three sampled reactors with a relative standard deviation <14%. (B) Butyrate experiment. Values presented in time points 0, 5, and 12 days represent the average of three sampled reactors with a relative standard deviation <20%.

correspond to the balance of the formed species during the oxidation.[17] At the initially adjusted circumneutral pH, the dissolved inorganic carbon corresponds to $H_2CO_3^*$ and HCO_3^-. $H_2CO_3^*$ can be expressed in terms of pCO_2 using Henry's law with its proportionality constant (k_H) corrected by temperature. The equations, as presented in Table 1, are deliberately written in terms of the H^+ concentrations and pCO_2 to illustrate the effect of these variables on the thermodynamic calculations.

ΔG_R^1 for the reactions presented above can be affected by pCO_2, pH, or by a combined interaction. The nature of the effect will depend on the role of the parameter in the catabolic reaction, meaning it acts as a reagent, product, or is not directly involved. As well, the magnitude of the effect might be amplified because of an initially less negative ΔG_R^{01}. A scenario analysis was performed to understand the impact of changing pCO_2 and pH on the ΔG_R^1 of the overall and intermediate catabolic reactions. The resulting calculations, subsequently, were used to estimate the change in the potential biochemical energy share. A summary of input parameters in each scenario (A, B, and C) is presented in Table S3, Supporting Information. The calculations were performed using a pH_2 value of 1×10^{-5} bar, typical for ADs[31] and at which syntrophic reactions become thermodynamically feasible.[17]

Statistical Analysis. Spearman's rank-order correlation coefficient (r_S) was calculated via the function rcorr() of the package "Hmisc" in R (v3.6.1),[28] ordered using hierarchical clustering and plotted using the package "corrplot."[32]

RESULTS AND DISCUSSION

Effect of Elevated pCO_2 on the Anaerobic Substrate Conversion and Metabolite Production Rate. Subplots A and C, as presented in Figure 1, show the decrease in substrate conversion rates in the experimental treatments at increased pCO_2 ranging from 0.3 to 8 bar during the 14 days. The reduction in r_{smax} was further quantified using the process parameters extracted from the data-fitting to the modified Gompertz equation, as presented in Table 2. Data from the 8 bar pCO_2 experiment are not included because it was not possible to determine the kinetic parameters accurately. Increasing pCO_2 from 0.3 to 5 bar led to a 93% reduction in r_{smax} for propionate, whereas for butyrate, the r_{smax} dropped by 57%. The calculated specific r_{smax} for propionate at 0.3 bar pCO_2 is already in the low range of the values proposed in the literature: 150−292 mg propionate g VSS^{-1} day^{-1}. In the case of butyrate, the specific r_{smax} at 0.3 bar pCO_2 was 1 order of magnitude lower than the inferior boundary of the theoretical range: 3.9−10.9 g butyrate g VSS^{-1} day^{-1}.[33] For both cases, elevated pCO_2 resulted in a concomitantly increase in the lag phase (λ), which is likely associated with inadequate levels of adaptation to operational conditions. A considerable effect on the production and consumption of acetate was not evident in

https://dx.doi.org/10.1021/acs.est.0c02022
Environ. Sci. Technol. 2020, 54, 12583−12592

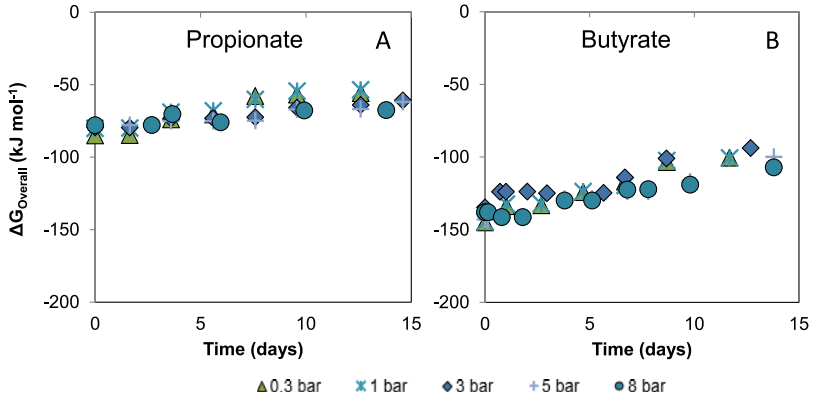

Figure 3. Change in the overall available Gibbs free energy ($\Delta G_{Overall}$) during mesophilic syntrophic (A) propionate oxidation and (B) butyrate oxidation at 0.3, 1, 3, 5, and 8 bar initial pCO_2 calculated with measured concentrations of reactants and products during the experimental period. Aqueous concentrations were used (in mol L^{-1}), the partial pressure of gases (in bar), T = 35 °C, and a theoretical value of $pH_2 = 1 \times 10^{-5}$ bar.

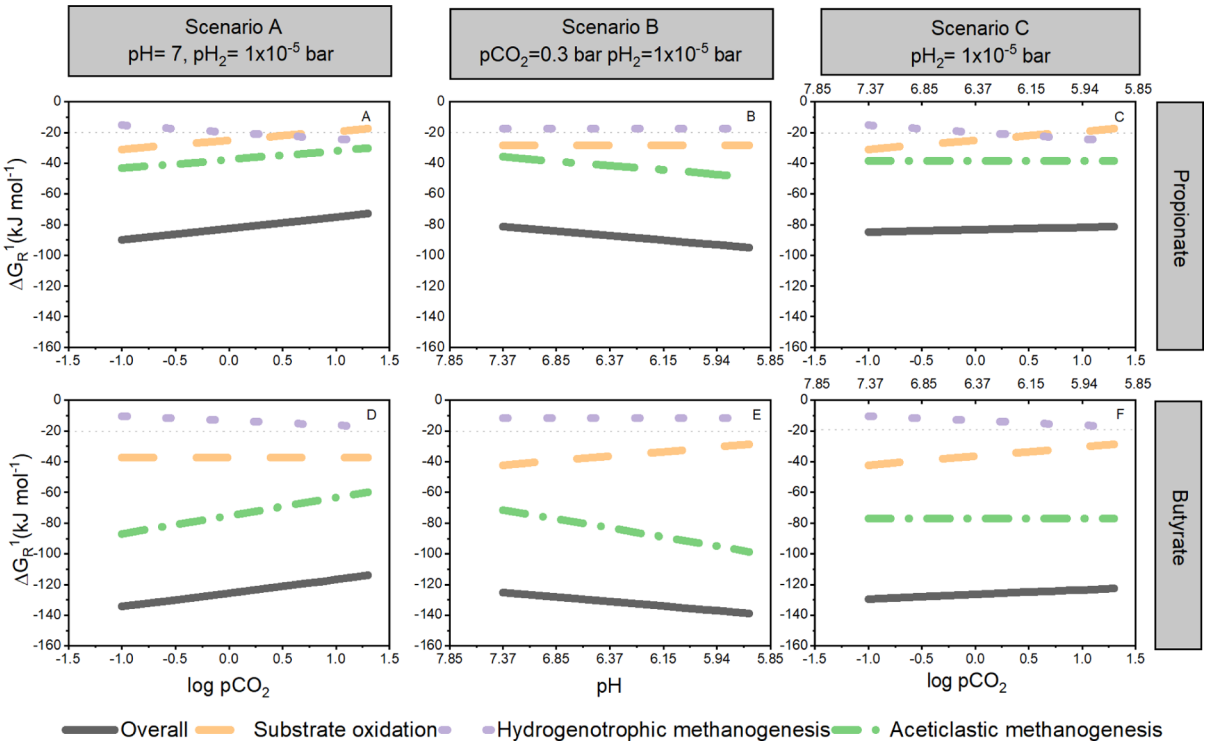

Figure 4. Effect of changing selected operational parameters on the ΔG_R^1 in the proposed scenarios for the syntrophic conversions. Scenario A—partial pressure of CO_2 (pCO_2) in propionate and butyrate conversion (A and D, respectively). Scenario B—pH in propionate and butyrate conversion (B and E, respectively). Scenario C—concomitant effect of pH and pCO_2 on propionate and butyrate conversion (C and F, respectively). Lines represent the ΔG_R^1 for the intermediate biochemical reactions: dotted-purple (HyM—ΔG_{HyM}), dashed-orange (oxidation of propionate—$\Delta G_{Pr\text{-}Ox}$ or butyrate—$\Delta G_{Bu\text{-}Ox}$), short-dash-dotted green (AcM—ΔG_{AcM}), and solid black (overall reaction—$\Delta G_{Overall}$). The experimental conditions (pH, pCO_2, and pH_2) that remained fixed during the calculation are included for reference in the upper part of the subplots. Values are presented as log pCO_2 for data linearization purposes. Concentrations of liquid reactants (mol L^{-1}) and gases (bar) correspond to the initial experimental conditions at T = 35 °C presented in the heading of Table S3, Supporting Information.

the propionate experiment; however, for butyrate, a decrease in acetate production occurred (Figure 1B,D). Lower methane production was observed in the propionate experiment only at 8 bar pCO_2 while it appeared already at 5 bar pCO_2 for butyrate (Figure 2A,B).

Hansson and Molin first reported the adverse effects of pCO_2 on the propionate and butyrate anaerobic conversion rate.[34] These authors observed a decrease of 70% in the r_{smax} in propionate degradation when increasing pCO_2 from 0.2 to 1 bar. The effect for butyrate was not significant, as opposed to our current work in which we identified an 18% reduction in r_{smax} at a comparable pCO_2 increase. In a previously reported experiment, using suspended pressure-cultivated inoculum that originated from anaerobic granular sludge degrading propionate,[5] it was shown that 5 bar pCO_2 caused a 93% reduction in the r_{smax}. This value agrees with the calculations presented here (Table 2).

Effects of Elevated pCO_2 on the $\Delta G_{Overall}$ of Syntrophic Propionate and Butyrate Conversion and the Intermediate Biochemical Reactions. Figure 3 shows the effect of applied pCO_2 on the overall available Gibbs free energy ($\Delta G_{Overall}$) during syntrophic propionate and butyrate

https://dx.doi.org/10.1021/acs.est.0c02022
Environ. Sci. Technol. 2020, 54, 12583−12592

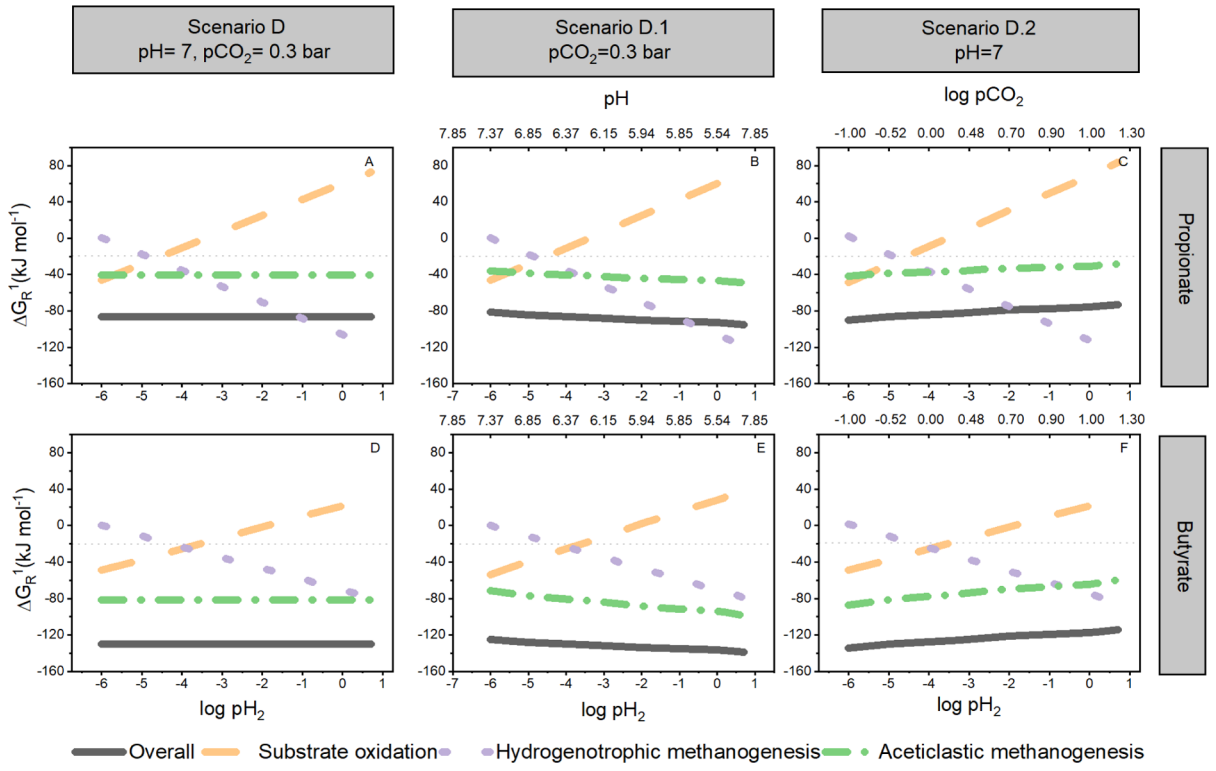

Figure 5. Effect of changing selected operational parameters on the ΔG_R^1 in the proposed scenarios for the syntrophic conversions. Scenario D—partial pressure of H_2 (pH_2) in propionate and butyrate (A and D, respectively). Scenario D.1—concomitant effect of pH and pH_2 in propionate and butyrate (B and E, respectively). Scenario D.2—concomitant effect of pH_2 and pCO_2 in propionate and butyrate (C and F, respectively). Lines represent the ΔG_R^1 for the intermediate biochemical reactions: dotted-purple (HyM—ΔG_{HyM}), dashed-orange (oxidation of propionate—$\Delta G_{Pr\text{-}Ox}$ or butyrate—$\Delta G_{Bu\text{-}Ox}$), short-dash-dotted green (AcM—ΔG_{AcM}), and solid black (overall reaction—$\Delta G_{Overall}$). The experimental conditions (pH, pCO_2, and pH_2) that remained fixed during the calculation are included for reference in the upper part of the subplots. Values are presented as log pCO_2 and log pH_2 for data linearization. Concentrations of liquid reactants (mol L^{-1}) and gases (bar) correspond to the initial experimental conditions at T = 35 °C presented in the heading of Table S3, Supporting Information.

conversion calculated using the actual concentrations of reactants during the atmospheric and pressure experiments and at $pH_2 = 1 \times 10^{-5}$ bar. Results showed a less steep increasing trend over time for $\Delta G_{Overall}$ from 1 bar pCO_2 onward, indicating that the two syntrophic reactions became less energetically feasible because of decreased substrate consumption or product accumulation. At day 0, the $\Delta G_{Overall}$ at 0.3 bar pCO_2 for propionate oxidation was −85.0, compared to −145.0 kJ mol^{-1} for butyrate oxidation. At 8 bar pCO_2, the $\Delta G_{Overall}$ for propionate increased to −78.0 compared to −137.9 kJ mol^{-1} for butyrate. The calculated dissimilarity in the $\Delta G_{Overall}$ of the reactions (≈40%) might have weakened the driving force to carry out propionate conversion at increased values of pCO_2 at atmospheric and pressurized conditions. This observation relates well with what Kleerebezem and Stams[18] proposed in their metabolic network analysis of syntrophic butyrate conversion, where they highlighted the possibility of a lowered specific reaction rate as a function of increased Gibbs free energy change of the catabolic reaction.

ΔG_R^1 responds to direct and indirect changes in biochemical reactions.[35] A deliberate change in the concentration of one or more biochemical species is considered a direct intervention. A change in the concentration of the species induced by the modification of another operational parameter is an indirect intervention. The predominance of a direct or indirect effect of increased pCO_2 on the $\Delta G_{Overall}$ and intermediate biochemical reactions of syntrophic conversions has not been thoroughly elucidated in literature. We tried to gain further insight into the individual and combined effects of elevated pCO_2 and pH on the bioenergetics using scenario analysis. By such analysis, possible bioenergetic limitations caused by an increase in the $\Delta G_{Overall}$ value might be identified.

Figure 4 visualizes the change in the ΔG_R^1 value when the parameters pCO_2 and pH are independently and concomitantly modified in syntrophic propionate and butyrate conversion. Lines represent the change in Gibbs free energy at increasing pCO_2 or decreasing pH for the intermediate biochemical reactions: substrate oxidation ($\Delta G_{Pr\text{-}Ox}$, $\Delta G_{Bu\text{-}Ox}$), AcM (ΔG_{AcM}), HyM (ΔG_{HyM}), and for the overall reaction ($\Delta G_{Overall}$). An increase in the $\Delta G_{Overall}$ in the subplots, as shown in Figure 4, means that less energy is available for all the subreactions, whereas a decrease implies that more energy is at hand. In scenario A, the $\Delta G_{Overall}$ for the syntrophic conversion of propionate and butyrate was calculated for an initial pCO_2 increasing from 0.1 to 20 bar to amplify the effect of elevated pCO_2 in comparison to our experimental range (0.3−8 bar). An elevated pCO_2 of 20 bar increased the $\Delta G_{Overall}$ of propionate by 19% and butyrate by 15%, compared to 0.1 bar (A and D). In scenario B, $\Delta G_{Overall}$ was calculated using the corresponding equilibrium pH values at pCO_2 ranging between 0.1 and 20 bar and buffer concentration of 100 mM as HCO_3^-. A pH change from 7.9 to 5.5 caused the $\Delta G_{Overall}$ to decrease by 14 and 10% for propionate and butyrate, respectively (B and E). In scenario C, $\Delta G_{Overall}$ was calculated with pCO_2 of scenario A and the pH values of scenario B. Under these

https://dx.doi.org/10.1021/acs.est.0c02022
Environ. Sci. Technol. 2020, 54, 12583−12592

conditions, there is a marginal increase in $\Delta G_{Overall}$ for the conversion of both substrates (C and F).

Concerning the intermediate reactions at 20 bar pCO_2 in scenario A, $\Delta G_{Pr\text{-}Ox}$ increased by 44%, and $\Delta G_{Bu\text{-}Ox}$ remained constant because CO_2 is not a reaction product. Regarding the methanogenic reactions, ΔG_{AcM} increased by 30%, whereas ΔG_{HyM} decreased by 40% for both substrates (A and D). The pH decrease to 5.5 in scenario B did not strongly affect the reactions where H^+ ions are not produced, that is, $\Delta G_{Pr\text{-}Ox}$ and ΔG_{HyM}. Contrastingly, $\Delta G_{Bu\text{-}Ox}$ increased by 32% and ΔG_{AcM} decreased by 27 and 28% for the propionate- and butyrate-fed assays, respectively, suggesting enhanced energetical feasibility of this reaction (B and E). In scenario C, $\Delta G_{Pr\text{-}Ox}$ and $\Delta G_{Bu\text{-}Ox}$ changed analogously to scenario A. ΔG_{AcM} remained the same in the entire pCO_2 range, which could be attributed to the simultaneous variation of pCO_2 annihilating the pH effects on the bioenergetics. The behavior of ΔG_{HyM} resembled scenario A because of the absent effect of H^+ production (C and F).

Scenario A highlighted the adverse effects of increased pCO_2 on the bioenergetics of syntrophic reactions. In this regard, Jin and Kirk[22] postulated that increasing pCO_2 from 0 to 30 bar in simulated non-buffered and buffered aquifer systems made SAO and AcM less energetically feasible, whereas the contrary was calculated for HyM. Moreover, they proposed additional effects of elevated pCO_2 on biochemical reactions because of induced changes in aqueous speciation, ionic strength, and in the reduction potential of redox couples such as H^+/H_2. Kato et al.[21] found that increasing pCO_2 from 0 to 1 bar strongly suppressed syntrophic activity in a model bacterial consortium for SAO, including the bacterium *Thermacetogenium phaeum* and the archaea *Methanothermobacter thermautotrophicus* and *Methanosaeta thermophila*. They established a 91% reduction in the r_{smax} of acetate, coincidently occurring when $\Delta G_{Ac\text{-}Ox}$ became higher than −20 kJ mol^{-1}, which is considered the smallest quantum to sustain life.[17] In our experiments, r_{smax} values decreased when pCO_2 increased from 0.3 to 8 bar, and the most significant drop also occurred when, theoretically, $\Delta G_{Pr\text{-}Ox}$ was higher than −20 kJ mol^{-1} (Supporting Information, Table S4).

Scenario B showed that decreasing pH modifies the bioenergetics of syntrophic propionate and butyrate conversion in a different direction than elevated pCO_2. Interestingly, pH can directly change the ΔG_R^1 when reactions produce or consume protons and indirectly as a result of modified chemical speciation.[35,36] From the bioenergetics point of view, proton (H^+)-consuming reactions, namely syntrophic oxidation and AcM (Table 1), could be promoted when decreasing pH inside a physiologically reasonable range. The more negative $\Delta G_{Overall}$ value in this scenario indicates a potential increase in the driving force to carry out the syntrophic reaction. Nonetheless, this might be compromised by physiological limitations and enhanced toxicity effects[37] observed at decreased pH levels, particularly in the case of methanogenic populations.[38] In consequence, bioenergetics does not suffice to elucidate the detrimental effects observed on the syntrophic conversions if pH is considered as the main explanatory variable.

Elevated pCO_2 as a Biochemical Steering Parameter. The distribution of available biochemical energy between the syntrophic partners is expected to change because of the direct and indirect effects of increasing pCO_2 on ΔG_R^1 of the overall and intermediate reactions (Supporting Information, Figure S3). In our results, the biochemical energy allocation is proposed under conditions of fixed pH_2. Under conditions of changing pH_2, pH, and pCO_2 (Figure 5, scenarios D, D.1, and D.2), a new thermodynamic equilibrium will be established, which can further modify the biochemical energy distribution among partners in syntrophic propionate and butyrate conversion. Values of pH_2 lower than 6×10^{-4} bar will have a positive effect on reaction feasibility, whereas higher values will reduce the feasibility "niche." The impact of increasing pH_2 on the available Gibbs free energy has been previously discussed in the literature;[39] nevertheless, its interaction with increased pCO_2 and decreased pH, to the best of our knowledge, has not been thoroughly described. A correlation analysis with hierarchical clustering of bioenergetic and experimental data was performed in order to verify whether the highlighted trends of the scenario analysis were still valid at a varying pH_2 (Supporting Information, Figure S4). Two theoretical values were chosen: a typical value for ADs at which syntrophic reactions are thermodynamically feasible (1×10^{-5} bar)[31] and the lowest detection level of the used gas chromatograph (6×10^{-4} bar). A strong negative correlation was found between pCO_2 and r_{smax} ($r_S = -0.82$, $p < 0.05$) for both propionate and butyrate. Concerning the Gibbs free energy change, a strong negative correlation was encountered only between $\Delta G_{Bu\text{-}Ox}$ and pH ($r_S = -0.78$, $p < 0.05$). ΔG_{AcM} was strongly negatively correlated with ΔG_{HyM} ($r_S = -0.87$, $p < 0.05$), evidencing the role of increasing pCO_2 and pH_2 in modulating the feasibility of methanogenic reactions.

Response of Syntrophic Anaerobic Conversion at Elevated pCO_2: Possible Physiological Effects. This study highlighted a possible relation between bioenergetic limitations and the observed kinetic effects occurring because of increased pCO_2. However, additional limitations cannot be discarded. For example, in our experiments, the dissolution of CO_2 from the headspace could decrease pH levels, irrespective of the applied high buffer concentration (100 mM HCO_3^-). Changes in pH disrupt cell homeostasis and impose limitations for growth, maintenance, and metabolic activity. In particular, syntrophic butyrate oxidizers (SBOs) and syntrophic propionate oxidizers (SPOs) demonstrate moderate growth at a pH lower than 6.5[40] and 6.0,[41] respectively. The increased lag phases and limited conversion under elevated pCO_2 could then be explained by the combination of pH effects on, for example, $\Delta G_{Bu\text{-}Ox}$ and physiological limitations affecting SBOs and SPOs at a different extent.

Also, the acidification of the fermentation medium modifies the equilibrium between undissociated and dissociated forms of the VFAs,[42] further altering cell homeostasis. At the applied pCO_2 of 8 bar and resulting equilibrium pH of 5.9, the concentrations of undissociated propionic acid (HPr) were slightly above inhibitory levels, that is, 20 mg L^{-1} HPr[43] (Supporting Information, Table S5). The concentration of undissociated butyric acid (HBu) remained below 500 mg L^{-1} HBu,[44] proposed in literature as inhibitory for growth in, for example, *Clostridium acetobutylicum*. Acetic acid concentrations (HAc) remained below indicative inhibitory levels in methanogenesis.[45] However, the detrimental effects of elevated pCO_2 in our experimental treatments were already seen at 1 bar pCO_2. Consequently, increased undissociated VFA concentrations do not explain the observed phenomena.

At elevated pCO_2, the equilibrium dissolved CO_2 concentration in the liquid medium increased from 320 to 8,620 mg L^{-1} (Supporting Information, Table S5). These dissolved CO_2 concentrations are in line with values reported by Wan et al.[10]

https://dx.doi.org/10.1021/acs.est.0c02022
Environ. Sci. Technol. 2020, 54, 12583−12592

(3,000−30,000 ppm), which negatively impacted the nitrogen removal efficiency because of increased membrane permeability, thus inhibiting electron transport and protein expression.

Furthermore, Salek et al.[46] showed that there is at least 1 order of magnitude difference in the kinetically controlled rate of physical reactions such as CO_2 dissolution and biochemical reactions, such as production of VFAs. This, in turn, may affect the concentration of the various species that are responsible for the reactions used in the thermodynamic calculations, leading to disparities in the calculated and observed bioenergetic effects at specific time points. More accurate pH_2 measurements in the low range, for example, $<6 \times 10^{-4}$ bar, are required to further validate the occurrence of the postulated effects on the feasibility of syntrophic reactions because of concomitant variation of pH_2 and pH or pCO_2. The possible role of other electron shuttles, whose appearance is favored by the presence of hydrogen and elevated pCO_2, particularly formate, needs to be further addressed.[47,48]

Elevated pCO_2 influences the kinetics and bioenergetics of the syntrophic conversion of propionate and butyrate. Based on this study, we propose that kinetic effects might appear as an evident sign of thermodynamic limitations, which is different for each compound. From detailed bioenergetic calculations, it was concluded that pCO_2 increases the $\Delta G_{Pr\text{-}Ox}$, induces pH changes that make $\Delta G_{Bu\text{-}Ox}$ more positive, and increases the $\Delta G_{Overall}$ of the syntrophic conversion. The more positive $\Delta G_{Overall}$ at elevated pCO_2 likely induces a redistribution of the available biochemical energy among the syntrophic partners that, if unbalanced, will translate into kinetic constraints. However, the here discussed biochemical energy limitations could not fully explain the strong kinetic effects on the system at increasing pCO_2. Presumably, the overall effects resulted from the concomitant impact of reduced thermodynamic feasibility, physiological effects associated with a lowered pH, and a minor detrimental impact of increased concentrations of undissociated VFAs. The observed kinetic and bioenergetic aftermath of elevated pCO_2 exposure might confer potentials for steering metabolic pathways, if limitations are overcome. For instance, the use of acclimated inocula[38] and energy-rich substrates such as sugars, proteins, or lipids could minimize the physiological impact of lowered pH and relieve bioenergetic limitations. Under such conditions, the steering potential of elevated pCO_2 on biochemical pathways in mixed culture anaerobic conversions could be unraveled.

■ ASSOCIATED CONTENT

Supporting Information

The Supporting Information is available free of charge at https://pubs.acs.org/doi/10.1021/acs.est.0c02022.

Role of inoculum origin on pCO_2 response; physicochemical characteristics of initial inocula; microbial community analysis, including Illumina sequencing protocol and absolute abundance results; sampling strategy; input parameters for the bioenergetics scenario analysis of syntrophic propionate and butyrate conversion; calculated values for $\Delta G_{Pr\text{-}Ox}$ in scenario A; theoretical share of $\Delta G_{Overall}$ for each of the proposed scenarios for the syntrophic conversion of propionate and butyrate; correlogram at different pH_2 values; and calculation of undissociated acids and carbonate equilibrium species for the anaerobic conversion experiments at 0.3, 1, 3, 5, and 8 bar pCO_2 (PDF)

■ AUTHOR INFORMATION

Corresponding Author

Pamela Ceron-Chafla − *Sanitary Engineering Section, Department of Water Management, Delft University of Technology, 2628 CN Delft, The Netherlands;* orcid.org/0000-0003-0437-6980; Email: p.s.ceronchafla@tudelft.nl

Authors

Robbert Kleerebezem − *Department of Biotechnology, Delft University of Technology, 2629 HZ Delft, Netherlands*

Korneel Rabaey − *Center for Microbial Ecology and Technology (CMET), Ghent University, B-9000 Ghent, Belgium; Center for Advanced Process Technology for Urban Resource Recovery (CAPTURE), B-9000 Ghent, Belgium;* orcid.org/0000-0001-8738-7778

Jules B. van Lier − *Sanitary Engineering Section, Department of Water Management, Delft University of Technology, 2628 CN Delft, The Netherlands*

Ralph E. F. Lindeboom − *Sanitary Engineering Section, Department of Water Management, Delft University of Technology, 2628 CN Delft, The Netherlands*

Complete contact information is available at: https://pubs.acs.org/10.1021/acs.est.0c02022

Notes

The authors declare no competing financial interest.

■ ACKNOWLEDGMENTS

This research was funded by European Union's Horizon 2020 research and innovation program under the Marie Skłodowska-Curie Grant Agreement No. 676070 (SuPER-W). This communication reflects only author's view, and the Research Executive Agency of the EU is not responsible for any use that may be made of the information it contains. Maria Gomez and Roberta Massini are acknowledged for their contributions to the experimental work.

■ NOMENCLATURE

ΔG_R^0	Gibbs free energy change for reaction R at standard temperature and pressure (kJ mol^{-1})
ΔG_R^{01}	Gibbs free energy change for reaction R corrected by biological pH reference value (pH = 7) (kJ mol^{-1})
ΔG_R^1	Gibbs free energy change for reaction R corrected by actual operational conditions (kJ mol^{-1})
$\Delta G_{Overall}$	Gibbs free energy change for the syntrophic reaction corrected by actual operational conditions (kJ mol^{-1})
$\Delta G_{Pr\text{-}Ox}$	Gibbs free energy change for propionate oxidation corrected by actual operational conditions (kJ mol^{-1})
$\Delta G_{Bu\text{-}Ox}$	Gibbs free energy change for butyrate oxidation corrected by actual operational conditions (kJ mol^{-1})
ΔG_{AcM}	Gibbs free energy change for aceticlastic methanogenesis corrected by actual operational conditions (kJ mol^{-1})
ΔG_{HyM}	Gibbs free energy change for hydrogenotrophic methanogenesis corrected by actual operational conditions (kJ mol^{-1})

https://dx.doi.org/10.1021/acs.est.0c02022
Environ. Sci. Technol. 2020, 54, 12583−12592

r_S Spearman's correlation coefficient[31]

REFERENCES

(1) Lindeboom, R. E. F.; Fermoso, F. G.; Weijma, J.; Zagt, K.; van Lier, J. B. Autogenerative High Pressure Digestion: Anaerobic Digestion and Biogas Upgrading in a Single Step Reactor System. *Water Sci. Technol.* **2011**, *64*, 647−653.

(2) Lemmer, A.; Chen, Y.; Lindner, J.; Wonneberger, A. M.; Zielonka, S.; Oechsner, H.; Jungbluth, T. Influence of Different Substrates on the Performance of a Two-Stage High Pressure Anaerobic Digestion System. *Bioresour. Technol.* **2015**, *178*, 313−318.

(3) Li, Y.; Liu, H.; Yan, F.; Su, D.; Wang, Y.; Zhou, H. High-Calorific Biogas Production from Anaerobic Digestion of Food Waste Using a Two-Phase Pressurized Biofilm (TPPB) System. *Bioresour. Technol.* **2017**, *224*, 56−62.

(4) Lindeboom, R. E. F.; Ferrer, I.; Weijma, J.; van Lier, J. B. Effect of Substrate and Cation Requirement on Anaerobic Volatile Fatty Acid Conversion Rates at Elevated Biogas Pressure. *Bioresour. Technol.* **2013**, *150*, 60−66.

(5) Lindeboom, R. E. F.; Shin, S. G.; Weijma, J.; van Lier, J. B.; Plugge, C. M. Piezo-Tolerant Natural Gas-Producing Microbes under Accumulating pCO_2. *Biotechnol. Biofuels* **2016**, *9*, 236.

(6) Spilimbergo, S.; Bertucco, A. Non-Thermal Bacteria Inactivation with Dense CO_2. *Biotechnol. Bioeng.* **2003**, *84*, 627−638.

(7) Manzocco, L.; Plazzotta, S.; Spilimbergo, S.; Nicoli, M. C. Impact of High-Pressure Carbon Dioxide on Polyphenoloxidase Activity and Stability of Fresh Apple Juice. *LWT–Food Sci. Technol.* **2017**, *85*, 363−371.

(8) Yu, T.; Chen, Y. Effects of Elevated Carbon Dioxide on Environmental Microbes and Its Mechanisms: A Review. *Sci. Total Environ.* **2019**, *655*, 865−879.

(9) Watanabe, T.; Furukawa, S.; Kawarai, T.; Wachi, M.; Ogihara, H.; Yamasaki, M. Cytoplasmic Acidification May Occur in High-Pressure Carbon Dioxide-Treated *Escherichia Coli*. *Biosci., Biotechnol., Biochem.* **2007**, *71*, 2522−2526.

(10) Wan, R.; Chen, Y.; Zheng, X.; Su, Y.; Li, M. Effect of CO_2 on Microbial Denitrification via Inhibiting Electron Transport and Consumption. *Environ. Sci. Technol.* **2016**, *50*, 9915−9922.

(11) Wan, R.; Chen, Y.; Zheng, X.; Su, Y.; Huang, H. Effect of CO_2 on NADH Production of Denitrifying Microbes via Inhibiting Carbon Source Transport and Its Metabolism. *Sci. Total Environ.* **2018**, *627*, 896−904.

(12) Mayumi, D.; Dolfing, J.; Sakata, S.; Maeda, H.; Miyagawa, Y.; Ikarashi, M.; Tamaki, H.; Takeuchi, M.; Nakatsu, C. H.; Kamagata, Y. Carbon Dioxide Concentration Dictates Alternative Methanogenic Pathways in Oil Reservoirs. *Nat. Commun.* **2013**, *4*, 1998.

(13) Xu, R.; Xu, S.; Florentino, A. P.; Zhang, L.; Yang, Z.; Liu, Y. Enhancing Blackwater Methane Production by Enriching Hydrogenotrophic Methanogens through Hydrogen Supplementation. *Bioresour. Technol.* **2019**, *278*, 481−485.

(14) Bajón Fernández, Y.; Soares, A.; Vale, P.; Koch, K.; Masse, A. L.; Cartmell, E. Enhancing the Anaerobic Digestion Process through Carbon Dioxide Enrichment: Initial Insights into Mechanisms of Utilization. *Environ. Technol.* **2019**, *40*, 1744−1755.

(15) Bajón Fernández, Y.; Green, K.; Schuler, K.; Soares, A.; Vale, P.; Alibardi, L.; Cartmell, E. Biological Carbon Dioxide Utilisation in Food Waste Anaerobic Digesters. *Water Res.* **2015**, *87*, 467−475.

(16) Al-mashhadani, M. K. H.; Wilkinson, S. J.; Zimmerman, W. B. Carbon Dioxide Rich Microbubble Acceleration of Biogas Production in Anaerobic Digestion. *Chem. Eng. Sci.* **2016**, *156*, 24−35.

(17) Schink, B. Energetics of Syntrophic Cooperation in Methanogenic Degradation. *Microbiol. Mol. Biol. Rev.* **1997**, *61*, 262−280.

(18) Kleerebezem, R.; Stams, A. J. M. Kinetics of Syntrophic Cultures: A Theoretical Treatise on Butyrate Fermentation. *Biotechnol. Bioeng.* **2000**, *67*, 529−543.

(19) Henze, M. *Biological Wastewater Treatment: Principles, Modelling and Design*; IWA Publishing, 2008.

(20) Leng, L.; Yang, P.; Singh, S.; Zhuang, H.; Xu, L.; Chen, W.-H.; Dolfing, J.; Li, D.; Zhang, Y.; Zeng, H.; Chu, W.; Lee, P.-H. A Review on the Bioenergetics of Anaerobic Microbial Metabolism Close to the Thermodynamic Limits and Its Implications for Digestion Applications. *Bioresour. Technol.* **2018**, *247*, 1095−1106.

(21) Kato, S.; Yoshida, R.; Yamaguchi, T.; Sato, T.; Yumoto, I.; Kamagata, Y. The Effects of Elevated CO_2 Concentration on Competitive Interaction between Aceticlastic and Syntrophic Methanogenesis in a Model Microbial Consortium. *Front. Microbiol.* **2014**, *5*, 575.

(22) Jin, Q.; Kirk, M. F. Thermodynamic and Kinetic Response of Microbial Reactions to High CO_2. *Front. Microbiol.* **2016**, *7*, 1696.

(23) Kirk, M. F. Variation in Energy Available to Populations of Subsurface Anaerobes in Response to Geological Carbon Storage. *Environ. Sci. Technol.* **2011**, *45*, 6676−6682.

(24) Jin, Q.; Bethke, C. M. The Thermodynamics and Kinetics of Microbial Metabolism. *Am. J. Sci.* **2007**, *307*, 643−677.

(25) Ghasimi, D. S. M.; Aboudi, K.; de Kreuk, M.; Zandvoort, M. H.; van Lier, J. B. Impact of Lignocellulosic-Waste Intermediates on Hydrolysis and Methanogenesis under Thermophilic and Mesophilic Conditions. *Chem. Eng. J.* **2016**, *295*, 181−191.

(26) American Public Health Association. *Standard Methods for the Examination of Water and Wastewater*; American Public Health Association, 2005.

(27) Do, H.; Lim, J.; Shin, S. G.; Wu, Y.-J.; Ahn, J.-H.; Hwang, S. Simultaneous Effect of Temperature, Cyanide and Ammonia-Oxidizing Bacteria Concentrations on Ammonia Oxidation. *J. Ind. Microbiol. Biotechnol.* **2008**, *35*, 1331−1338.

(28) R Core Team. *R: A Language and Environment for Statistical Computing*, 2019. https://www.r-project.org/.

(29) Kleerebezem, R.; Van Loosdrecht, M. C. M. A Generalized Method for Thermodynamic State Analysis of Environmental Systems. *Crit. Rev. Environ. Sci. Technol.* **2010**, *40*, 1−54.

(30) Heijnen, J. J.; Kleerebezem, R. Bioenergetics of Microbial Growth. *Encyclopedia of Industrial Biotechnology*; Wiley, 2010; pp 1−66.

(31) Patón, M.; Rodríguez, J. A Compilation and Bioenergetic Evaluation of Syntrophic Microbial Growth Yields in Anaerobic Digestion. *Water Res.* **2019**, *159*, 176−183.

(32) Wei, T.; Simko, V. *R Package "corrplot": Visualization of a Correlation Matrix*, version 0.84, 2017. https://github.com/taiyun/corrplot.

(33) van Lier, J. B.; Mahmoud, N.; Zeeman, G. Anaerobic Wastewater Treatment. *Biological Wastewater Treatment: Principles, Modelling and Design*; IWA Publishing, 2008; pp 401−442.

(34) Hansson, G.; Molin, N. End Product Inhibition in Methane Fermentations: Effects of Carbon Dioxide and Methane on Methanogenic Bacteria Utilizing Acetate. *Eur. J. Appl. Microbiol. Biotechnol.* **1981**, *13*, 236−241.

(35) Jin, Q.; Kirk, M. F. pH as a Primary Control in Environmental Microbiology: 2. Kinetic Perspective. *Front. Environ. Sci.* **2018**, *6*, 101.

(36) Bethke, C. M.; Sanford, R. A.; Kirk, M. F.; Jin, Q.; Flynn, T. M. The Thermodynamic Ladder in Geomicrobiology. *Am. J. Sci.* **2011**, *311*, 183−210.

(37) Ali, S.; Hua, B.; Huang, J. J.; Droste, R. L.; Zhou, Q.; Zhao, W.; Chen, L. Effect of Different Initial Low pH Conditions on Biogas Production, Composition, and Shift in the Aceticlastic Methanogenic Population. *Bioresour. Technol.* **2019**, *289*, 121579.

(38) Mao, C.; Feng, Y.; Wang, X.; Ren, G. Review on Research Achievements of Biogas from Anaerobic Digestion. *Renewable Sustainable Energy Rev.* **2015**, *45*, 540−555.

(39) De Kok, S.; Meijer, J.; Van Loosdrecht, M. C. M.; Kleerebezem, R. Impact of Dissolved Hydrogen Partial Pressure on Mixed Culture Fermentations. *Appl. Microbiol. Biotechnol.* **2013**, *97*, 2617−2625.

(40) Balk, M.; Altinbas, M.; Rijpstra, W. I. C.; Sinninghe Damste, J. S.; Stams, A. J. M. *Desulfatirhabdium Butyrativorans* Gen. Nov., Sp. Nov., a Butyrate-Oxidizing, Sulfate-Reducing Bacterium Isolated from an Anaerobic Bioreactor. *Int. J. Syst. Evol. Microbiol.* **2008**, *58*, 110−115.

https://dx.doi.org/10.1021/acs.est.0c02022
Environ. Sci. Technol. 2020, 54, 12583−12592

(41) Li, J.; Ban, Q.; Zhang, L.; Jha, A. K. Syntrophic Propionate Degradation in Anaerobic Digestion: A Review. *Int. J. Agric. Biol.* **2012**, *14*, 843−850.
(42) Xiao, K.; Zhou, Y.; Guo, C.; Maspolim, Y.; Ng, W. J. Impact of Undissociated Volatile Fatty Acids on Acidogenesis in a Two-Phase Anaerobic System. *J. Environ. Sci.* **2016**, *42*, 196−201.
(43) Maillacheruvu, K. Y.; Parkin, G. F.; Ma, K. Y. Kinetics of Growth, Substrate Utilization and Sulfide Toxicity for Propionate, Acetate, and Hydrogen Utilizers in Anaerobic Systems. *Water Environ. Res.* **1996**, *68*, 1099−1106.
(44) Monot, F. d.; Engasser, J.-M.; Petitdemange, H. Influence of pH and Undissociated Butyric Acid on the Production of Acetone and Butanol in Batch Cultures of *Clostridium Acetobutylicum*. *Appl. Microbiol. Biotechnol.* **1984**, *19*, 422−426.
(45) Xiao, K. K.; Guo, C. H.; Zhou, Y.; Maspolim, Y.; Wang, J. Y.; Ng, W. J. Acetic Acid Inhibition on Methanogens in a Two-Phase Anaerobic Process. *Biochem. Eng. J.* **2013**, *75*, 1−7.
(46) Salek, S. S.; van Turnhout, A. G.; Kleerebezem, R.; van Loosdrecht, M. C. M. pH Control in Biological Systems Using Calcium Carbonate. *Biotechnol. Bioeng.* **2015**, *112*, 905−913.
(47) Oswald, F.; Stoll, I. K.; Zwick, M.; Herbig, S.; Sauer, J.; Boukis, N.; Neumann, A. Formic Acid Formation by *Clostridium Ljungdahlii* at Elevated Pressures of Carbon Dioxide and Hydrogen. *Front. Bioeng. Biotechnol.* **2018**, *6*, 6.
(48) Roger, M.; Brown, F.; Gabrielli, W.; Sargent, F. Efficient Hydrogen-Dependent Carbon Dioxide Reduction by *Escherichia Coli*. *Curr. Biol.* **2018**, *28*, 140−145.

https://dx.doi.org/10.1021/acs.est.0c02022
Environ. Sci. Technol. 2020, 54, 12583−12592